ORIGINAL RESEARCH ARTICLE

Can multiple fish farms be integrated within a semi-enclosed bay without causing acute ecosystem degradation?

Kristian Puhr [a,*], Kristina Pikelj [b], Željka Fiket [c]

[a] Department of Biology, Faculty of Science, University of Zagreb, Zagreb, Croatia
[b] Department of Geology, Faculty of Science, University of Zagreb, Zagreb, Croatia
[c] Division for Marine and Environmental Research, Ruđer Bošković Institute, Zagreb, Croatia

Summary   The current study explores the possibility that multiple fish farms (FFs) containing sea bass (*Dicentrarchus labrax*) and sea bream (*Sparus aurata*) can be successfully integrated within a semi-enclosed bay in the Croatian Adriatic. The research focuses on determining principal environmental factors (EFs) that control the integration and attempts to estimate their individual and synergic ability to influence deposition and removal of organic matter (OM) and trace elements (TE) from the system. The complexity of the designated tasks demanded a comprehensive number of various datasets and samples to be used in the analysis. The ADCP data revealed strong wind induced currents forming within the research domain resulting in high system flushing efficiency (3.5—6 days). The sediment samples from all stations contained relatively inert minerals which contributed to overall low OM and TE concentrations and very limited variability found across the entire bathymetric range. The thermal advection effect recorded at two stations was attributed to specific seabed topography and the hydrodynamic response formed during *Maestral* wind episodes. The results indicate that a successful integration of four FFs has taken place within the research site (semi enclosed bay), and that the key EFs responsible for its success are strong wind induced hydrodynamics, favorable seabed topography and sediment mineral composition. The synergy of the principal EFs that formed within the

* Corresponding author at: Department of Biology, Faculty of Science, University of Zagreb, Rooseveltov trg 6, 10 000 Zagreb, Croatia.
Tel.: +385 91 502 77 92; fax: +385 1 3380 676.
  E-mail addresses: kristian.puhr@gmail.com (K. Puhr), kpikelj@geol.pmf.hr (K. Pikelj), zeljka.fiket@irb.hr (Ž. Fiket).

system was found to have an attenuating effect regarding FFs chemical influence (OM and TE) and an amplifying one regarding spatial footprint which extended to ≈2000 m distance.

1. Introduction

The aquaculture industry has rapidly increased in the Mediterranean region over the past two decades (Apostolaki et al., 2009) and this trend is expected to continue. Fish farming (FF) of sea bass (*Dicentrarchus labrax*) and sea bream (*Sparus aurata*) has had the greatest annual growth rate of all aquaculture production types in the Croatian Adriatic (FAO FishstatJ, 2012). The excessive production of organic matter (OM) and certain trace elements (TE) typically associated with this type of industry (Cancemi et al., 2003; Delgado et al., 1997; Wu, 1995) caused significant concerns, due to the enclosed nature of the Adriatic basin. Although extensive research has already been conducted to elucidate the fish farming short term and long term effects, various aspects of aquaculture influence still require comprehensive investigation and description. The majority of the results point to a conclusion that FFs generate a negative biochemical pressure on the surrounding environment, though on relatively small spatial scales (Karakassis et al., 2000; Pergent-Martini et al., 2006). However, some scientific papers have reported that farming of sea bass and sea bream within the oligotrophic Mediterranean could be considered as tolerable for the ecosystem pending key environmental factors (EFs) support the integration (Karakassis et al., 2005; Maldonado et al., 2005; Puhr and Pikelj, 2012). The current study used the latter approach as a scientific foundation and went further by analyzing the ecological impact of multiple FFs located within a semi-enclosed bay in the Croatian Adriatic. Similar interactions between multiple aquaculture installations and a semi-enclosed system have been previously studied in the East Mediterranean with results having indicated medium to low impact on the ecosystem's nutrient stability (Neofitou and Klaoudatos, 2008; Papageorgiou et al., 2010). The first priority of the research was to determine the principal EFs that control the deposition and removal of OM and TE within the research site. These had to be primarily derived from *in situ* measurements as their scales of influences vary depending on site specific properties (Borja et al., 2009). Once identified, the principal EFs serve as a basis for investigating their synergic power which is expected to develop due to the enclosed nature and relative shallowness of the research site. This phenomenon is of particular interest as very little is known about its capabilities to amplify or attenuate aquaculture impacts. The complexity of the designated tasks demanded a comprehensive number of various datasets and samples to be used in the analysis. The datasets consisted of: *in situ* light and water temperature measurements, meteorological records of wind direction, intensity and air temperature, Eulerian current measuring device data (ADCP), and hydrographic data on seabed topography.

Sediment samples were gathered *in situ* and analyzed for grain size, carbonate content, quartz, OM and TE content. Upon completion, the results of the study were expected to answer two very important questions: (1) can multiple FFs be integrated within a semi-enclosed bay without causing acute ecosystem degradation, and (2) are the prerequisites for a successful integration dependent on highly improbable combination of site-specific environmental factors or rather on set of conditions commonly found in numerous locations throughout the East Adriatic and the Mediterranean Sea?

2. Material and methods

2.1. Study area

The study area is located on the island of Ugljan (East Adriatic Sea, Zadar Archipelago, Croatia) and covers app. 2800 m × 1500 m section of the southern part of the island, including two large enclosed bays (Vela Lamjana and Mala Lamjana) and four small islands (Fig. 1). The entire area, which can be regarded as a semi-enclosed bay, comprises of 4 fish farming installations (containing sea bass and sea bream) and a small shipyard, making this location potentially susceptible to eutrophication and heavy metal toxicity. The site is partly exposed to *Jugo* (SSE-ESE) and *Maestral* (WNW-NW) winds, and is sheltered from *Bura* (NNE-ENE) wind which causes the wind driven hydrodynamics to be relatively attenuated. Seabed topography can be described as favorable due to the specific layout of the islands and the two enclosed bays (Fig. 1). From the geological point of view, the island of Ugljan belongs to the Zadar Islands group and is composed of thick-bedded Cretaceous limestones and Eocene foraminiferal limestones (Majcen et al., 1970). The seabed around the islands has a recognizable biogenic coarse-grained carbonate-rich surface sediment cover (Pikelj et al., 2016).

2.2. Data from the meteorological station

The meteorological data corresponding to the time interval of the *in situ* field measurement were obtained from the National Meteorological and Hydrological Service (DHMZ) Station in Zadar (10 km N of the research site). Wind speed [m s^{-1}] and direction (00-32) were recorded every 10 min by the sensor placed 2 m above the ground (7 m above sea level). Average values were then calculated to express prevailing wind direction and intensity for each hour of the day. Air temperature values were recorded in °C every hour by the thermograph.
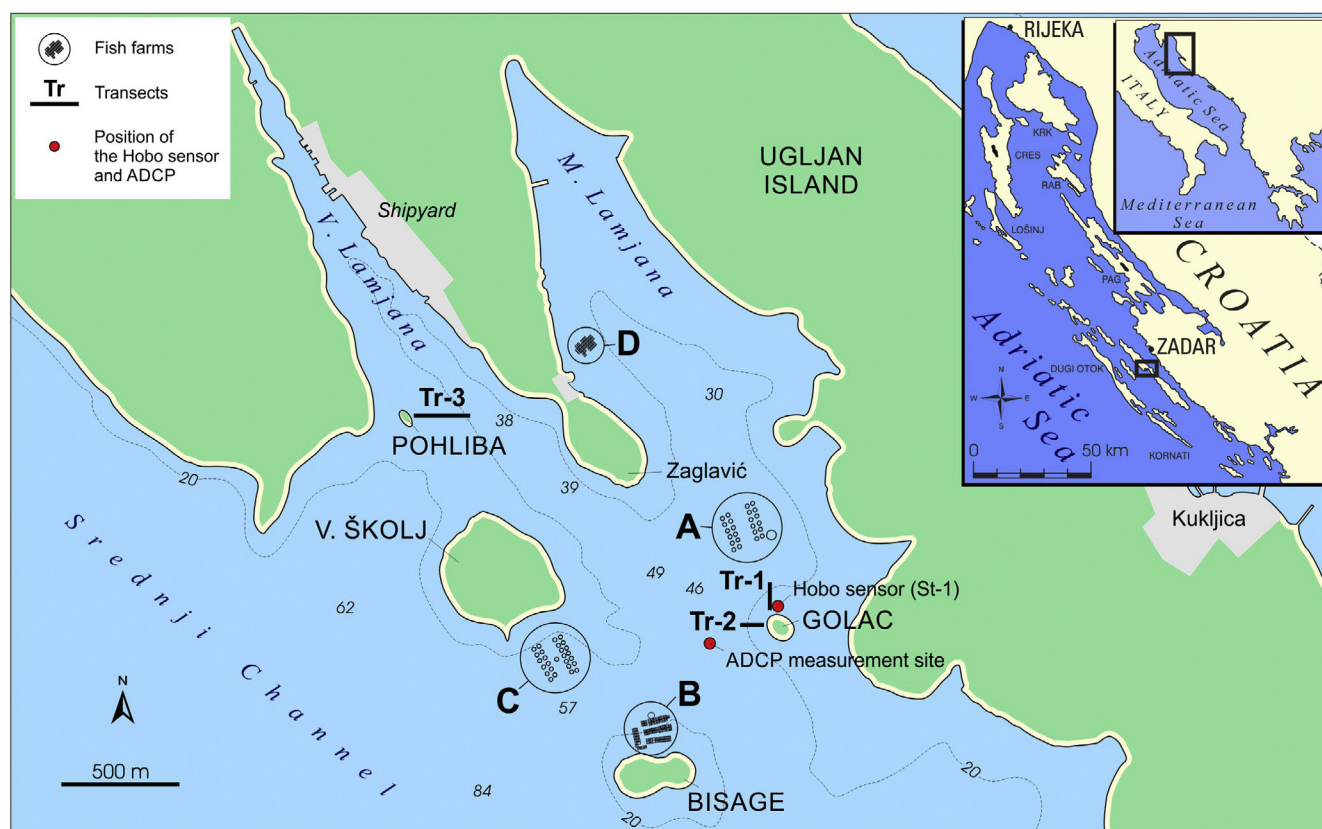
Figure 1 Map of the research area. A semi-enclosed system consisting of two fully enclosed bays (V. Lamjana and M. Lamjana) and four islands (Pohliba, V. Školj, Bisage and Golac).

2.3. *In situ* deployed sensors

2.3.1. Light intensity and water temperature

Light intensity (lux) and water temperature measurements [°C] were continuously recorded every 15 min *in situ* using ONSET Hobo Pendant® Temperature/Light Data Logger with an accuracy of ±0.01 lux and ±0.47°C. The bottom sensor (S1) was anchored with a vertical iron bar pushed deep into the sediment at a depth of 5 m at St-1 (Fig. 1). The subsurface (S2) sensor was immersed 10 cm and tied to a rope connecting the anchor with the surface buoy positioned directly above S1 sensor. The attenuation coefficient of scalar irradiance (K_d) was calculated from the difference in recorded data of S1 and S2 sensors by applying Beer—Lambert exponential decay function: $(I_z = I_o e^{-K_d z})$ $K_d = -\text{Ln} (I_z/I_o) z^{-1}$ where K_d is the light attenuation coefficient in units of $[m^{-1}]$, I_z is light measured at depth z, and I_o is light measured just under the surface. In order to average out the eventual data anomalies, such as variable sun angle (Miller and McPherson, 1995) or stochastic pulsed turbidity events (Longstaff and Dennison, 1999), 7 day average values of the light intensity readings taken between 10:00 and 17:00 h of each day were used in calculation.

2.3.2. Current measurements and hydrodynamic modeling

Sea currents have been measured from July 23rd till September 9th 2007 for the purpose of evaluating the potential impact of a new fish farming installation in the Lamjana bay area (SUO Lamjana, 2011). The Eulerian current measuring device (ADCP) was placed at a depth of 45 m about 50 m SW from the end of the Tr-2 transect (Fig. 1). By using statistical analysis, the acquired data were transformed into average vectors and scale values, necessary for modeling surface and bottom water layer movements within the research area. Using the 3D hydrodynamic model (Princeton Ocean Model; Blumberg and Mellor, 1987) it was possible to create a simulation of the current movements depending on the direction and the intensity of the wind. The horizontal resolution of the model was 50 m, and the water column was divided into 11 uneven layers, having an increased resolution close to the surface and the sea bottom. The results of the hydrodynamic simulation model were used in the estimation of two very important temporal parameters: (1) residence time, and (2) flushing time. Since in the marine environment, nutrients, contaminants, dissolved gases, and suspended particles are carried passively in a fluid medium, it is essential to define hydrodynamic processes that transport water and its constituents. The first-order description of transport within a boundary defined area is expressed as "residence time" or "flushing time" (Monsen et al., 2002). Residence time is defined as amount of time required for a water parcel at any given location of an embayment to leave the boundaries of that embayment (Takeoka, 1984). Flushing time defines the amount of time required to replace a defined water mass or introduced material in a coastal system. In the simulation, flushing time is expressed as the time required to remove 63% of the initially introduced material in the

embayment (Knauss, 1978), meaning that at the end of the flushing time period ($t = T_f$) about $1/e$ (37%) of the initial mass of the material still remains in the system. Both residence time and flushing time were estimated using specially designed software called *PartTrak3* at the Institute of Oceanography and Fisheries in Split.

2.4. Sediment sampling and analyses

2.4.1. Sediment sampling
The data acquisition was performed at 3 stations (St-1, St-2, and St-3) within the bay using SCUBA dive method of stratified sampling along the depth gradient with predetermined azimuth (transects perpendicular to the shore, starting from the station points). Station 1 (St-1, Tr-1) was located approx. 120 m south (S) from the fish farm "A", Station 2 (St-2, Tr-2) was approx. 550 m (NE) from fish farm "B" and approx. 800 m (E) from fish farm "C", and Station 3 (St-3, Tr-3) was positioned at the entrance to the V. Lamjana bay where the small shipyard is located (Fig. 1). St-1 was chosen for two principle reasons: (1) its proximity to fish farming influence (transect 1 (Tr-1) ended only 20 m away from the cages), and (2) for having an almost linear increase in bathymetric values with no underwater thresholds or depressions between the cages and the shoreline. St-2 is situated much further from the primary source of influence, and has an underwater depression separating the two fish farms (B and C) from the shoreline of the island of Golac where both stations (St-1 and St-2) are located. St-3 is positioned at the eastern shore of the island of Pohliba, and was primarily chosen to measure the influence of the shipyard on the area outside the V. Lamjana bay. Transects were oriented N (Tr-1), W (Tr-2) and E (Tr-3) respectively (Fig. 1), and sediment samples were taken using: (a) plastic and inox corers (20 cm long and 4.5 cm wide) inserted vertically into the sediment, and (b) plastic containers (0.15 L) horizontally pushed to remove top 3—5 cm of sediment. Samples were taken at 2 m, 5 m, 10 m, 15 m, 20 m, and 25 m depth. After the extraction, all samples were frozen immediately at −20°C and transported to the lab. Prior to analyses, sediment samples were defrosted and air dried. Surface sediments stored in plastic containers were homogenized and powdered, then separated into subsamples for carbonate content, OM content, major (ME) and trace (TE) elements assessment. Due to the general coarseness of the sediments and the absence of vertical change in grain size, the core samples were also gently homogenized and used for grain size analysis in order to obtain enough material of mud fraction for sedigraph technique. We used two replicates for each analysis performed.

2.4.2. Grain size analysis
From each sample 150—200 g of dried sediment were weighed and wet sieved using 7 ASTM standard stainless sieves (from >4 mm to <0.063 mm). Suspension containing particles <0.063 mm was prepared and analyzed by Sedigraph 5100, following standard Micromeritics Sedigraph procedure. Sediment texture and statistical granulometrical parameters were identified and calculated according to Folk's (1954) classification scheme by using Gradistat package (Blott and Pye, 2001). After grain size analysis, coarse (gravel and sand) fractions were microscopically examined for qualitative bulk identification of sediment particles. Special attention was given to quartz particles identification, especially in sediments sampled at transects Tr-1 and Tr-2. Since there was no natural source of quartz on land surrounding the research site it was assumed that the origin of this mineral could only be attributed to shipyard's sand blasting activities (Fajković et al., 2013; SUO Lamjana, 2011).

2.4.3. Carbonate content
Amounts of carbonate in all of the powdered bulk samples were determined using Scheibler apparatus for gas volumetry (standard: HRN ISO: 10693:2004). This method is based on the volumetric evolution of carbon dioxide after reaction of carbonates with dilute (1:1) hydrochloric acid. Carbonate content of each sample was determined in duplicate, and the results represent the average value of the two measurements.

2.4.4. Organic matter (OM) content
OM content was determined through the weight loss on ignition (LOI). Ceramic crucibles were cleaned with distilled water, dried and weighed. Approximately 2 g of fine powdered sediment were placed in the crucibles which were reweighed. Crucibles with sediment were heated at 500°C for 6 h and the percent of LOI was estimated as the difference of mass of crucibles with sediment before and after the combustion. In order to ensure analytical precision, each sample was analyzed twice and the results represent the average values of the two individual estimates.

2.4.5. Levels of major (ME) and trace (TE) elements
All samples were analyzed for total concentration of 29 elements (Al, As, Ba, Be, Bi, Cd, Co, Cr, Cs, Cu, Fe, K, Li, Mg, Mn, Mo, Na, Ni, Pb, Rb, Sb, Sn, Sr, Ti, Tl, U, V, Zn and Zr). Prior to analysis, sediment subsamples (0.1 g) were subjected to total digestion in the microwave oven (Multiwave 3000, Anton Paar, Graz, Austria) in two-step procedure consisting of digestion with a mixture of 4 mL nitric acid (HNO_3) − 1 mL hydrochloric acid (HCl) − 1 mL hydrofluoric acid (HF) followed by addition of 6 mL of boric acid (H_3BO_3). Each solution was transferred to a precleaned plastic volumetric flask and diluted to 100 mL. Prior to analysis, samples were further diluted 2-fold, acidified with 2% (v/v) HNO_3 (65%, supra pur, Fluka, Steinheim, Switzerland) and indium (In, 1 μg L^{-1}) was added as internal standard. The multi-element analysis of prepared samples was performed by High Resolution Inductively Coupled Plasma Mass Spectrometry (HR ICPMS) using an Element 2 instrument (Thermo, Bremen, Germany). The typical instrument condition and measurement parameters used throughout the work can be found in the available literature (Cukrov et al., 2008; Fiket et al., 2016). Standards (solutions) were prepared by appropriate dilution of a multi-elemental reference standard (Analytika, Prague, Czech Republic) containing Al, As, Ba, Be, Bi, Cd, Co, Cr, Cs, Cu, Fe, Li, Mn, Mo, Ni, Pb, Rb, Sr, Ti, Tl, V and Zn in which single element standard solutions of U (Aldrich, Milwaukee, WI, USA), Sn (Analytika, Prague, Czech Republic) and Sb (Analytika, Prague, Czech Republic) were added. For determining Zr, a single reference standard (Alfa Aesar, Germany) was used, whereas the determination of ME (Na, K and Mg) was based on multi-elemental reference standard (Fluka, Germany). Quality control of analytical procedure was

performed by simultaneous analysis of blank and certified reference material (CRM) for marine sediment (MESS-3, National Research Council Canada, Ontario, Canada). For all measured elements the average procedural blank readings were at least two orders of magnitude lower than the element concentrations in sediment sample solutions, and in accordance with those previously published by Fiket et al. (2016). Exceptions were Be, Bi and Sb for which the solution element concentrations differed only by an order of magnitude compared to blank values. Good agreement between the analyzed and certified concentrations (within their analytical uncertainties) was obtained for all elements ($\pm 10\%$).

2.4.6. Statistical analyses

The ME and TE data were later treated statistically using SigmaPlot 11.0 and Statistica 7 software for Windows. Analysis of variance (ANOVA) on ranks and subsequent pair-wise comparison by Dunn's method was applied to test the differences between the levels of measured elements at different sampling sites, with the level of significance set at $p < 0.05$. Chemometrical characterization of the sediments samples was done using principal component analysis (PCA). The significance of differences ($p < 0.05$) between groups of sediments, including sediments sampled along individual transects, was determined by nonparametric Kruskal—Wallis test for analysis of variance (ANOVA).

3. Results

3.1. Temperature measurements

The air temperature and sea water temperature measurements display different trends in daily oscillations. Air temperature values show a predictable (Gaussian like) distribution

(Fig. 2), while sea water temperatures show sudden increases and decreases during 24 h periods (Fig. 3). This fluctuation pattern was found to be highly correlated to *Maestral* wind which occurs from late spring to early autumn months as a result of high atmospheric pressure (anticyclone) and insolation. On the days that *Maestral* wind was blowing (5.07.—7.7.2013, and 10.07.—11.07.2013), a clear sudden temperature increase (1.5°C/15 min) occurred regularly around 14:00 h (Fig. 3), which can be attributed to wind driven thermal advection (Puhr and Pikelj, 2012). The water temperature readings from the days when *Bura* wind was influencing the hydrodynamics of the area (8.07.—9.07.2013) show a different 24 h oscillation, having two peaks (first around 12:00 h, second around 16:00 h) and much smaller temperature variations.

3.2. Wind direction and intensity

The analysis of the wind direction and intensity log revealed two predominant winds (*Maestral* and *Bura*) blowing during the time interval of *in situ* measurements. With *Maestral* as predominant wind, the wind intensity distribution shows a predictable pattern, having a steady increase from 08:00 h in the morning, reaching its peak around 14:00 h, and then having a slow and steady decrease in the afternoon. For periods with *Bura* as predominant wind, the intensity distribution shows a relatively constant influence from early morning till midnight, with the highest intensity values measured between 08:00—09:00 h and 10:00—11:00 h. The important difference between the two winds is the variability of wind forcing in time, and the subsequent hydrodynamic response which is strongly influenced by the frequency of the forcing and the effect of the coast in relation to wind direction (Orlić and Pasarić, 2011).
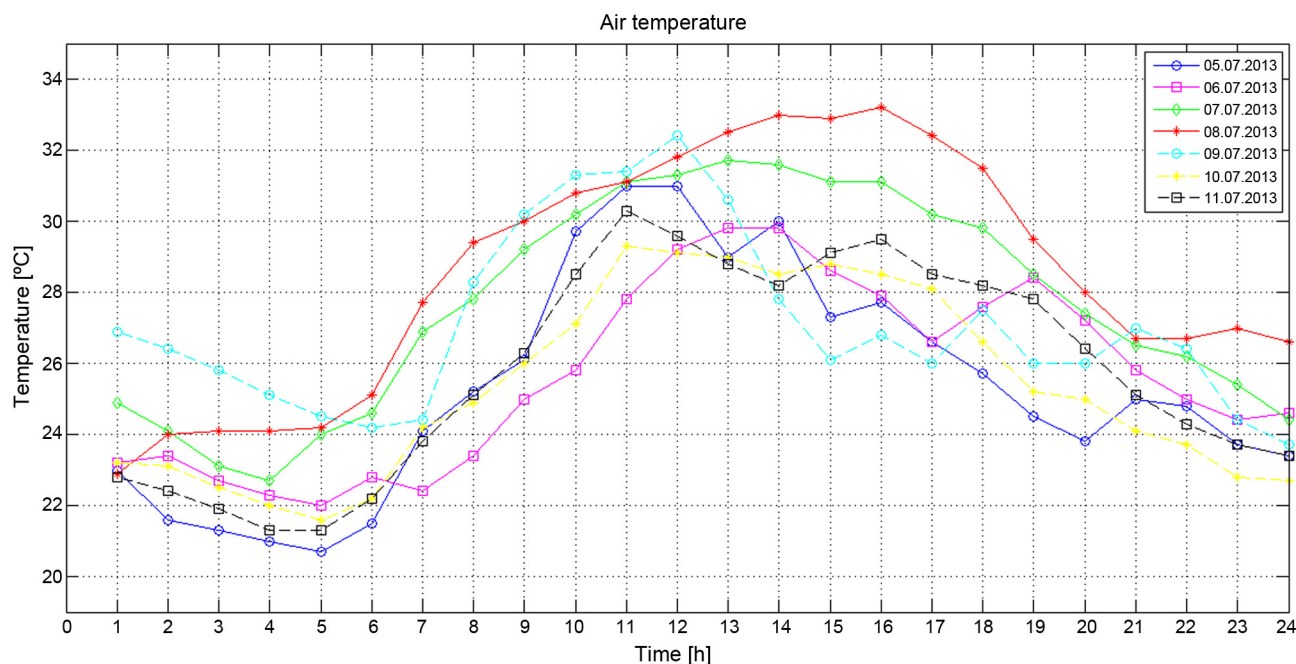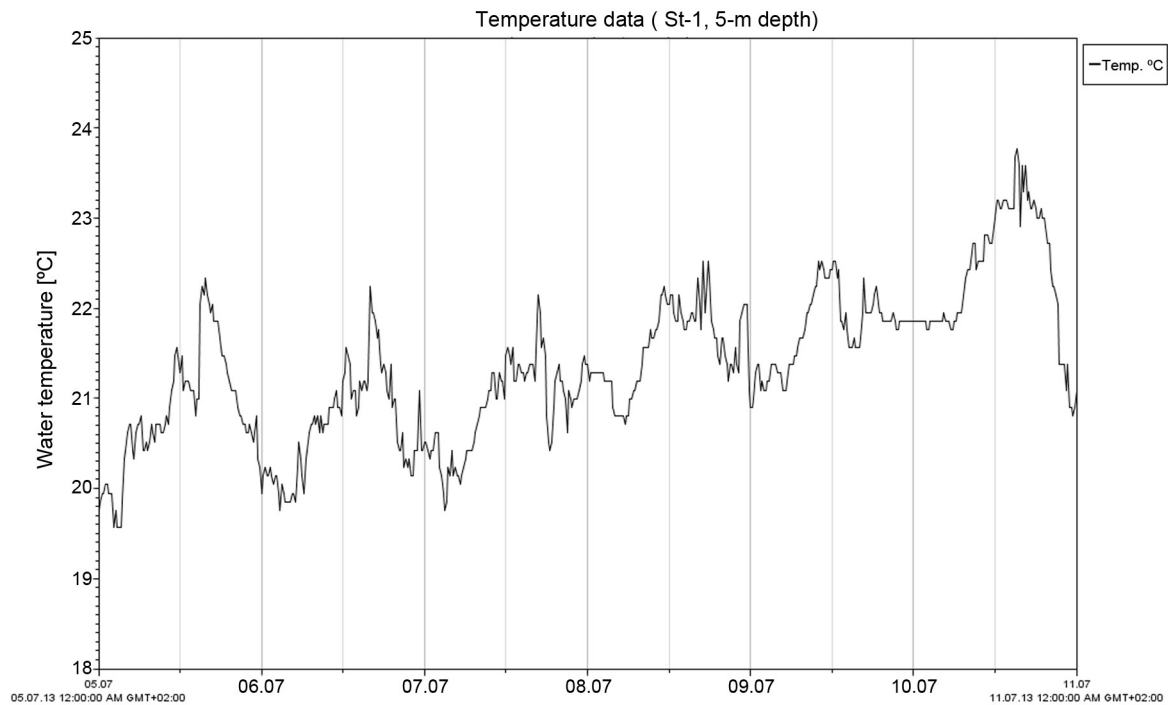

Figure 2 Air temperature graph [24 h measurement/7 days].

Figure 3 Sea temperature readings taken between 05.07.2013 and 11.07.2013, measured continuously every 15 min. The dates indicated at [x] axes represent values measured at midnight. The peaks show a sudden temperature increase caused by wind-induced thermal advection during *Maestral* periods.

3.3. Light intensity measurements

The attenuation coefficient K_d was calculated from average values recorded by S1 and S2 sensors between 9.00 and 17.00 h each day in the period of 7 days. The measured K_d value of 0.149 is higher than expected but within limits for a semi-enclosed system strongly affected by wind induced water mixing.

3.4. Sediment analysis

3.4.1. Sediment grain size
The sampled sediments are generally classified as poorly (or very poorly) sorted sands (Table 1), with sand fraction constituency varying between 65% and 93%. Gravelly sands (gS) occur at the shallowest depths (2 m and 5 m) at all three transects, with the exception of transect Tr1 where gravelly

Table 1 Summarized descriptive statistics of studied sediment variables along each transect.

Sample	Sampling depth [m]	Sediment type (Folk, 1954)	Mean grain size [μm]	Sorting [phi]	Gravel [%]	Sand [%]	Silt + clay [%]	Carbonates [%]	Organic matter [%]
Transect 1 (Tr1)									
Tr1-2	2	gS	539	1.77	10.1	83.2	5.6 + 1.1	88.3	2.1
Tr1-5	5	gS	510	1.682	9.0	85.7	4.8 + 0.5	91.4	2.5
Tr1-10	10	gS	457	1.806	9.2	84.1	5.6 + 1.1	89.6	2.1
Tr1-20	20	gmS	236	2.081	5.2	78.2	14.9 + 1.7	76.1	2.7
Tr1-25	25	(g)mS	163	1.552	2.6	84.5	12.2 + 0.7	61.5	2.6
Transect 2 (Tr2)									
Tr2-5	5	gS	885	2.134	28.8	64.5	6.0 + 0.7	95.3	2.5
Tr2-10	10	gS	658	1.833	16.6	79.2	3.5 + 0.7	87.1	2.8
Tr2-20	20	(g)S	325	1.633	3.9	89.8	5.5 + 0.8	83.7	2.8
Tr2-25	25	(g)S	207	1.487	2.2	93.1	4.3 + 0.4	61.0	1.8
Transect 3 (Tr3)									
Tr3-2	2	gS	590	1.824	13.4	80.8	5.2 + 0.6	94.2	3.5
Tr3-5	5	gS	649	1.252	6.4	90.1	2.9 + 0.6	97.1	2.5
Tr3-10	10	gmS	422	1.979	6.8	81.9	10.1 + 1.2	93.7	2.7
Tr3-15	15	(g)S	296	1.755	3.8	86.8	8.8 + 0.6	93.8	3.7
Tr3-20	20	gmS	266	2.403	7.4	72.7	17.5 + 2.4	82.2	4.1

sand was sampled at 10 m depth (Table 1). The mean grain sizes (Mz) of gravelly sands vary between medium and coarse sand (457—885 μm). The percentage of gravel in samples varies from 2 to 29, and shows a sudden decrease in sediments collected deeper than 10 m depth (Table 1). The apparent increase of the amount of mud (silt + clay) with increasing depth (≥10 m) is observable only along transect Tr1, while transects Tr2 and Tr3 do not show recognizable pattern along the depth gradient. Sediment samples containing highest mud share (>10%) are characterized as gravelly muddy sands (gmS) or slightly gravelly muddy sands ((s) gmS). Sediments sampled at higher depths containing <10% of mud are classified as slightly gravelly sands ((s)gS) (Table 1). Consequently, the mean sizes of sediments from the deepest part of transects display lower values compared to the shallow sediment cover: they vary between fine and medium sands (163—422 μm), mostly due to the lower proportion of gravel and/or the higher proportion of mud. On the individual level, each transect shows a gradual sediment fining with increasing depth, recognizable through the change in the mean grain size. The main granulometric differences along each transect are visible in the percentage of gravel and mud fraction changes (Table 1). Gravel and sand fractions of all the studied sediments mostly contain carbonate biogenic particles (skeletons, shells and shell fragments). Molluscan fragments dominate the gravel and very coarse sand fractions in the majority of samples. Echinoids are minor contributors to these fractions, while carbonate litoclasts significantly contribute in sediments collected along transect Tr2. Gastropods and bivalves are major skeletal components in coarse and medium coarse sand, while echinoids, foraminifera, worm tubes, bryozoans, and sponge spicules are present to a lesser extent. Foraminifera, sponge spicules and ostracod carapaces dominate in fine and very fine sands. Quartz was identified in samples from all stations and was dominant in very fine sands and silt fraction of the deeper sampled sediments from transects Tr1 and Tr2. The fact that quartz was identified in sediments over 2000 m away from the source expands the shipyard's radius of influence over the fish farms at locations A, B and C (Fig. 1).

3.4.2. Carbonate content

All analyzed sediments are carbonate-rich, and have carbonate content ranging between 61% and 97%. The general decreasing trend in carbonate content with increasing depth is evident along each transect (Table 1). The widest range of carbonates occurs in sediments along transect Tr2 ($\Delta \sim 34\%$), and a slightly smaller difference is noted along transect Tr1 ($\Delta \sim 30\%$). Transect Tr3 has consistent high carbonate content values throughout the bathymetric range ($\Delta \sim 15\%$).

3.4.3. Organic matter (OM) content

The OM contents have shown relatively uniform values along studied transects, ranging between 1.8% and 4.1% in all sediment samples. Transect Tr1 has the narrowest range, between 2.1% and 2.7%, while transect Tr2 had a slightly wider range, between 1.8% and 2.8%. Transect Tr3 has the widest OM content range, with values between 2.5% and 4.1%.

3.4.4. The levels of major (ME) and trace elements (TE) in sediments

The concentrations of measured elements in the studied sediment samples are listed in Table 2. Fig. 4 displays the distribution of concentrations of selected elements within the studied sediments. The obtained concentrations show variability between sediments of individual transects, as well as within each transect. For elements Al, Ba, Co, Cr, Cs, K, Li, Mn, Rb, Sb, Ti, Tl, and Zr, an increase along all three transects, from shallower to deeper parts, by a factor of 3—7, was observed. The lowest variability in the composition was observed for sediments along transect Tr2, whereas the highest concentrations for most of these elements were observed in sediment sampled at a maximum depth (25 m) of transect Tr1. For elements As, Be, Cu, Fe, Pb, Sn and Zn an increase in concentration along transects Tr1 and Tr3 was observed, while the same elements show very little variation along transect Tr2. The highest values of As, Be, Cu, Fe, Pb, Sn and Zn were observed in sediment sampled at maximum depth (20 m) of transect Tr3, being 2 to 6 times higher than the highest value measured in the other two transects (Tr1 and Tr2). The concentrations of Mo and, to a lesser extent, of Bi, Ni and V are decreasing with increasing depth in the sediments of transect Tr2, whereas along two other transects an increase in concentrations of these elements was observed. Only for Mg and Cd a decrease in concentrations, from shallower to deeper parts, along each of the three transects was observed. The overall lowest spatial variability was obtained for U (11%) and Sr (16%). Due to variability in grain-size composition and carbonate content, differences between sediments were investigated using normalized concentrations, with Li used as a reference element. The element mostly used for marine sediment normalization is aluminum (Al), since it represents aluminosilicates — the main group of minerals generally found in the fine sediment fractions. However, due to the sporadic occurrences of *terra rossa* on the island of Ugljan, which contains a high proportion of aluminum, it was decided that lithium (Li) would serve as a better normalizing element. Normalized concentrations of Al, Cs, K and Rb display little variability between sediments of individual transects, as well as along each transect, while Cr, Ti, and Zr show an increase in normalized concentrations with increasing depth along all three transect, having the highest values in sediment sampled at the deepest part (25 m) of transect Tr1. Normalized concentrations of As, Be, Cu, Fe, Sn and Zn show different trends in the sediments of individual transects. Lowest variability of normalized concentrations was observed for these elements along transects Tr1, while in sediments of transect Tr2 more intense decline, from shallower to deeper parts, was observed. Only along transect Tr3 an increase of normalized concentrations was observed for these elements, with the highest values measured in sediment sampled at the greatest depth (20 m), suggesting a more intense increase in concentrations than expected given the granulometric characteristics. Only for Cd, Mg, Sr and U, a decrease of normalized concentrations with depth along all three transects was observed.

3.4.5. Statistical analyses

The results of the PCA, which show the correlation between concentrations of elements in sediments and the first three

Table 2 Concentrations of elements [mg kg^{-1}] in sediments along each transect.

Sample	Al	As	Ba	Be	Bi	Cd	Co	Cr	Cs	Cu	Fe	K	Li	Mg
Transect 1														
Tr1-2	1074	2.23	11.6	0.03	0.01	0.12	0.29	34.3	0.104	1.30	852	733	2.67	10,269
Tr1-5	979	2.01	11.7	0.02	0.01	0.09	0.22	18.5	0.104	1.30	658	697	2.11	8226
Tr1-10	1753	1.53	12.0	0.03	0.02	0.08	0.30	43.7	0.158	1.28	923	933	2.95	6917
Tr1-20	3353	1.80	24.1	0.06	0.03	0.06	0.66	93.5	0.332	2.22	1881	1603	5.09	5353
Tr1-25	5383	3.81	47.7	0.13	0.05	0.07	0.93	126	0.477	3.04	2971	2187	7.95	8509
Transect 2														
Tr2-5	1359	2.32	12.6	0.04	0.03	0.13	0.45	18.4	0.148	1.52	1500	793	2.73	9209
Tr2-10	2582	1.66	17.3	0.09	0.03	0.10	0.55	24.2	0.293	3.05	1443	1535	4.55	11,890
Tr2-20	2277	1.72	17.7	0.05	0.02	0.07	0.54	42.5	0.249	1.81	1384	1292	4.07	10,036
Tr2-25	3276	2.08	34.5	0.08	0.03	0.06	0.58	64.2	0.317	2.01	1606	1638	6.38	7380
Transect 3														
Tr3-2	1454	2.34	14.2	0.06	0.02	0.08	0.40	10.9	0.183	3.01	1288	1009	3.45	12,784
Tr3-5	1498	2.51	13.4	0.09	0.02	0.06	0.35	10.4	0.202	2.53	1310	717	3.48	9871
Tr3-10	2973	5.60	23.8	0.09	0.04	0.05	0.59	22.3	0.339	3.64	2816	1101	4.79	5068
Tr3-15	1929	7.48	21.8	0.10	0.04	0.06	0.65	25.5	0.230	4.04	2572	1014	3.87	8449
Tr3-20	4572	13.43	78.1	0.34	0.07	0.09	1.66	72.8	0.505	11.4	5554	1880	7.11	9789

	Mn	Mo	Ni	Pb	Rb	Sb	Sn	Sr	Ti	Tl	U	V	Zn	Zr
Transect 1														
Tr1-2	57.7	0.504	2.13	5.64	1.70	0.106	1.29	1704.2	208.8	0.025	1.15	8.51	8.86	11.3
Tr1-5	40.1	0.309	2.13	6.34	1.66	0.074	1.07	1655.3	177.4	0.027	1.10	6.68	19.6	14.8
Tr1-10	32.1	0.348	2.49	5.56	2.92	0.097	1.61	1979.8	273.9	0.023	1.35	7.55	5.77	24.9
Tr1-20	78.3	0.390	4.15	8.33	5.70	0.156	1.18	1732.5	650.1	0.063	1.27	10.1	14.8	54.9
Tr1-25	195	0.520	5.33	10.7	9.37	0.257	1.50	1496.7	1110.0	0.100	1.38	13.9	15.7	84.1
Transect 2														
Tr2-5	74.9	1.29	3.34	9.11	2.11	0.168	0.866	1437.7	175.2	0.031	1.56	13.0	22.1	12.1
Tr2-10	69.1	0.878	5.04	9.51	4.44	0.169	2.18	1781.5	291.2	0.054	1.50	11.6	12.6	27.8
Tr2-20	99.5	0.641	4.46	8.41	3.96	0.175	1.15	2028.5	288.9	0.051	1.55	8.52	9.81	28.9
Tr2-25	102	0.448	3.32	9.86	6.55	0.232	0.942	1265.4	763.7	0.077	1.37	9.43	9.71	49.1
Transect 3														
Tr3-2	72.6	0.526	2.63	10.1	2.54	0.111	1.37	2049.7	106.5	0.053	1.40	7.49	14.5	16.1
Tr3-5	43.5	0.554	2.37	9.75	2.66	0.106	1.33	2068.8	120.3	0.060	1.55	9.45	16.2	14.2
Tr3-10	63.2	0.526	5.31	10.1	4.72	0.169	1.23	2096.2	270.0	0.069	1.49	12.8	12.2	28.9
Tr3-15	115	0.694	4.51	11.9	3.31	0.165	1.54	2200.7	168.6	0.085	1.31	12.3	21.7	19.4
Tr3-20	189	1.02	6.81	21.7	7.53	0.306	4.16	2095.5	524.2	0.105	1.52	25.9	47.9	55.2

components (PC1, PC2 and PC3), are presented in Fig. 5. The first two principal components explained 79.4% of the total variability, with PC1 and PC2 accounting for 59.1% and 20.3% of the total variance, respectively. On the negative side of the first component (PC1), Al, Ba, Bi, Co, Cs, Li, Mn, Ni, Rb, Sb, Tl and V have the greatest effect (>0.87) (Fig. 5a). The fact that Al, Cs, Li and Rb are the major constituents of detrital minerals points to a conclusion that the content of elements related to the first component (PC1) reflects the geological background, and includes those elements which are enhanced. The strongest contribution for PC2 was obtained for carbonate content. Since the coarseness of the studied sediments is primarily influenced by the original size of shells and shell fragments, it seems logical to assume that PC2 reflects the particle size distribution. PC3 explained additional 7.0% of the total variance, with Sr having the greatest negative effect on PC3 (0.63) and Cd having the greatest positive effect on PC3 (0.82) (Fig. 5b). Since a large share of strontium in carbonates is caused by substitution of

Ca with Sr in the crystal lattice, strontium can be considered as an indicator of biogenic components within sediments (Morse and Mackenzie, 1990). The nonparametric Kruskal—Wallis test showed that there is a statistically significant difference ($p < 0.05$) between sediments of different transects for only several elements (As, Cu, Pb, Sr and U).

3.5. Hydrodynamic modeling

3.5.1. Currents profiling
The results of the simulations show that hydrodynamics of the area are significantly influenced by the wind direction and thermal stratification of the water column. The numerical experiment for 4 m s^{-1} *Maestral* wind and thermally stratified water column shows strong influence in the subsurface layer with currents being forced along the shoreline in the basin, especially increasing water transport around the islands V. Škoj and Bisage. The bottom currents are generally of lower intensity except for the shallow part of
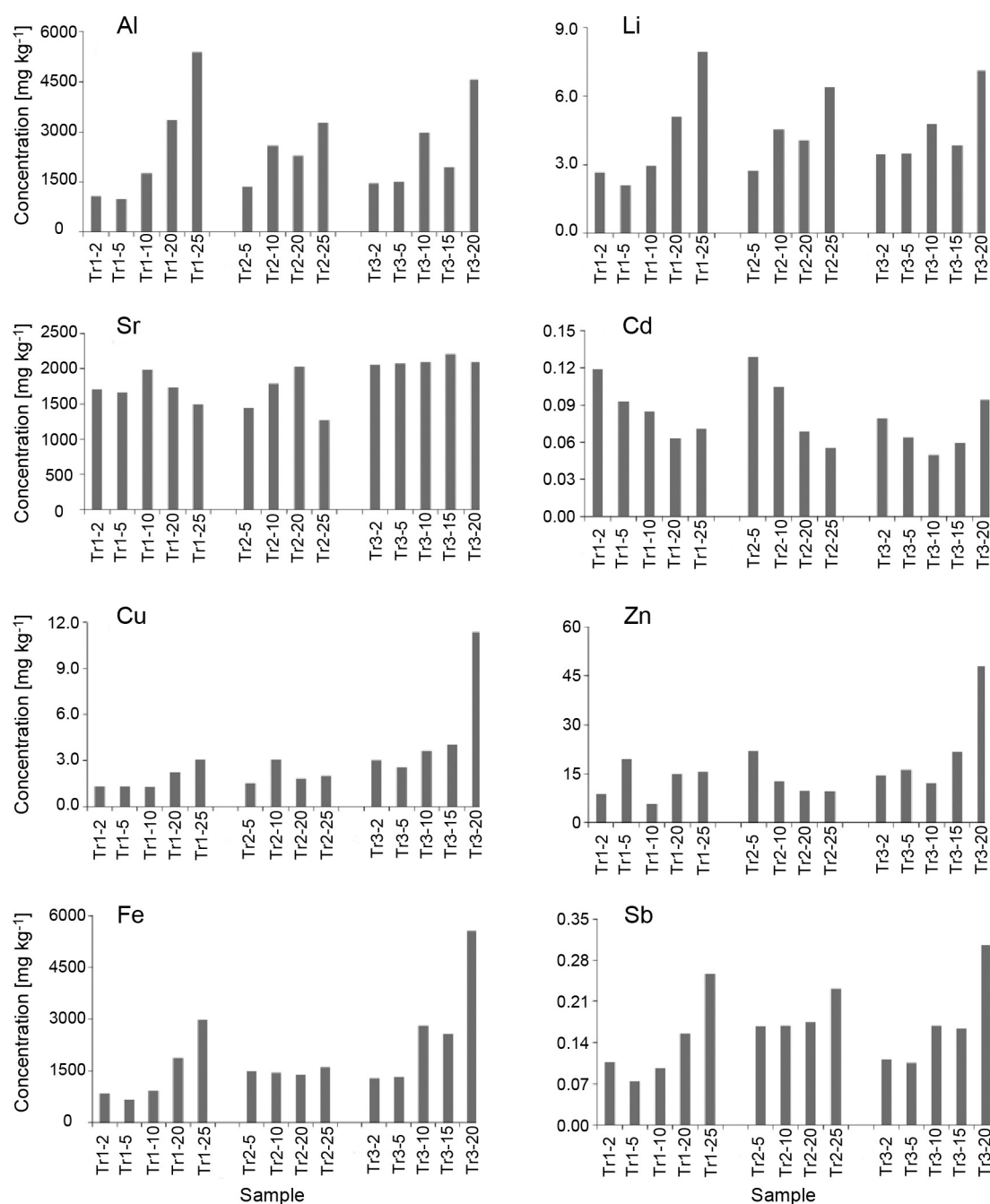
Figure 4   The concentration of selected elements [mg kg^{-1}] obtained from samples taken at predetermined depths.

the M. Lamjana bay. The simulation for *Bura* wind with average speed of 5 m s^{-1} and vertically homogeneous sea shows a different hydrodynamic influence across the bathymetric range. The subsurface current is flowing at an angle of 45° to the right from the wind direction, with exception inside the shallow parts of the bays and around the islands Golac and Bisage. The bottom current acts as a compensation current flowing in opposite direction with slightly lower intensity. In the simulations, the wind speeds of 5 m s^{-1} for *Bura* and 4 m s^{-1} for *Maestral* were used as these values represent typical wind intensity averages for the Middle Adriatic climatologic zone (SUO Lamjana, 2011).

3.5.2. Residence time and flushing time estimations
The estimations for residence time and flushing time are displayed in Fig. 6. For *Maestral* wind, the simulation shows relatively short residence time within the central part (islands) and V. Lamjana bay area, and high residence time values for M. Lamjana bay and shallow eastern coastal area (Fig. 6a). The island of Golac has a slightly elevated residence time in the area of Tr-1 (St-1). Flushing time representation displays three different values: the graphical representation (T_f) displays dots which represent 5% decrease in the concentration ratio between starting number of particles and the particles left in the simulation domain after a specified
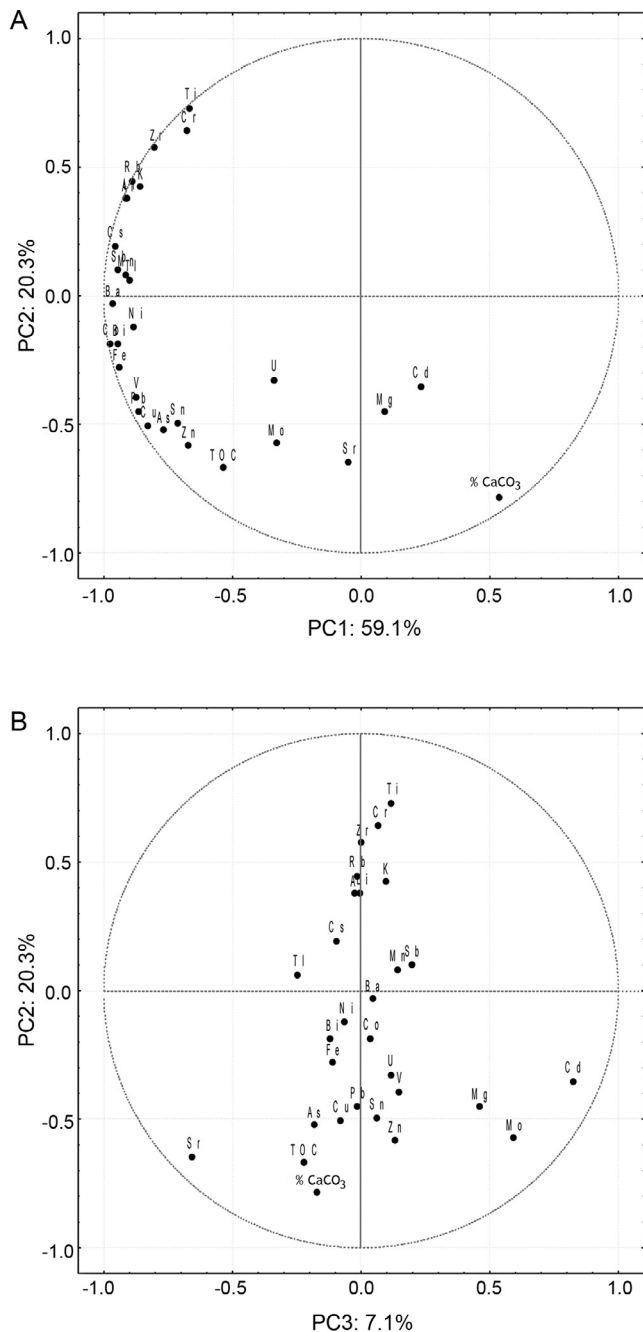
Figure 5 Principal component analysis. (A) Loading plot of principal components PC1 and PC2, (B) loading plot of principal components PC1 and PC3.

time period, and from these points in the graph two functions (r_1 and r_2) are calculated using simple linear regression, resulting in mathematical flushing time estimations (T_{f1} and T_{f2}). The T_{f1} and T_{f2} values are displayed in the graphs as two lines (exponential) intersecting with a horizontal line at some point in time. The horizontal line represents the point in time where about $1/e$ (37%) of the initial mass of the introduced material still remains in the system. From the three values (T_f, T_{f1} and T_{f2}) the most probable value is calculated as an arithmetic middle (SUO Lamjana, 2011). For the *Maestral* wind, the simulation displays an average flushing time of approximately 6 days (Fig. 6b). The computer

estimation of *Bura* wind residence time shows a favorable hydrodynamic influence within the entire simulation domain, except in M. Lamjana bay and the north-western part of V. Lamjana bay where residence time values are high (Fig. 6c). The average flushing time is approximately 3.5 days (Fig. 6d), corresponding to almost half the value of the estimated flushing time for the *Maestral* wind, which is surprising since the entire research area is well protected from first quadrant winds and therefore expected to have longer residence time and higher flushing time values for *Bura* wind episodes.

4. Discussion

4.1. Principal environmental factors (EFs)

The results of the present study promote wind induced hydrodynamics, favorable seabed topography and sediment mineral composition as principal EFs that control the system's capacity to process and eliminate scalars introduced by the industries occupying the research site. Wind driven hydrodynamics were identified as the dominant EF from two different sources: the ADCP data and the sediment samples. The ADCP datasets were used in synthesizing simulation models which clearly revealed strong currents forming within the research domain. Flushing time estimations of 3.5 and 6 days (Fig. 6) are indicative of a highly efficient scalar removal system responsible for keeping the semi-enclosed bay relatively unaffected by the FFs presence. The simulation models results were verified by examining the sediment OM and TE values both individually and collectively. The OM concentration, a principal indicator of FF activity and an important factor for scavenging metals (Förstner and Wittmann, 1983), was found to have surprisingly low values considering the semi-enclosed nature of the site and the presence of multiple fish farming installations. The average OM value in Mid-Adriatic fine-grained sediments containing more than 75% of sand fraction is less than 2% (Matijević et al., 2008), and as the investigated sediment samples ware coarse-grained and carbonate-rich (Table 1), the measured OM content values from collected samples can be classified as elevated, but not high. Although Transect Tr-1 was the closest to the primary source of OM (Fish farm A; Fig. 1) and undoubtedly experienced continuous input, the OM levels within the entire bathymetric range showed surprisingly low values and very limited variability, even at deeper transect points where sediments contain >10% of silt and clay fraction. This uniformity highly correlates with intensive flushing within the entire water column thus confirming the simulation models accuracy. The levels of TE display similar pattern with low variability across the depth gradient (except the deepest point of Tr-3). The analysis revealed slightly elevated concentrations of elements Cu, Zn, Fe, Cd and Pb within samples from transects Tr-1 and Tr-3. This was to be expected as specified elements are typically related to fish farming (Clement et al., 2010; Pergent et al., 1999) and shipyard activities (Karlsson et al., 2010). However, although slightly elevated, their concentrations when compared to their average Mid Adriatic values (Dolenec et al., 1998) seem unusually low. The overall low concentrations of both OM and TE promote wind induced hydrodynamics as being the principal force that controls the dilution and subsequent
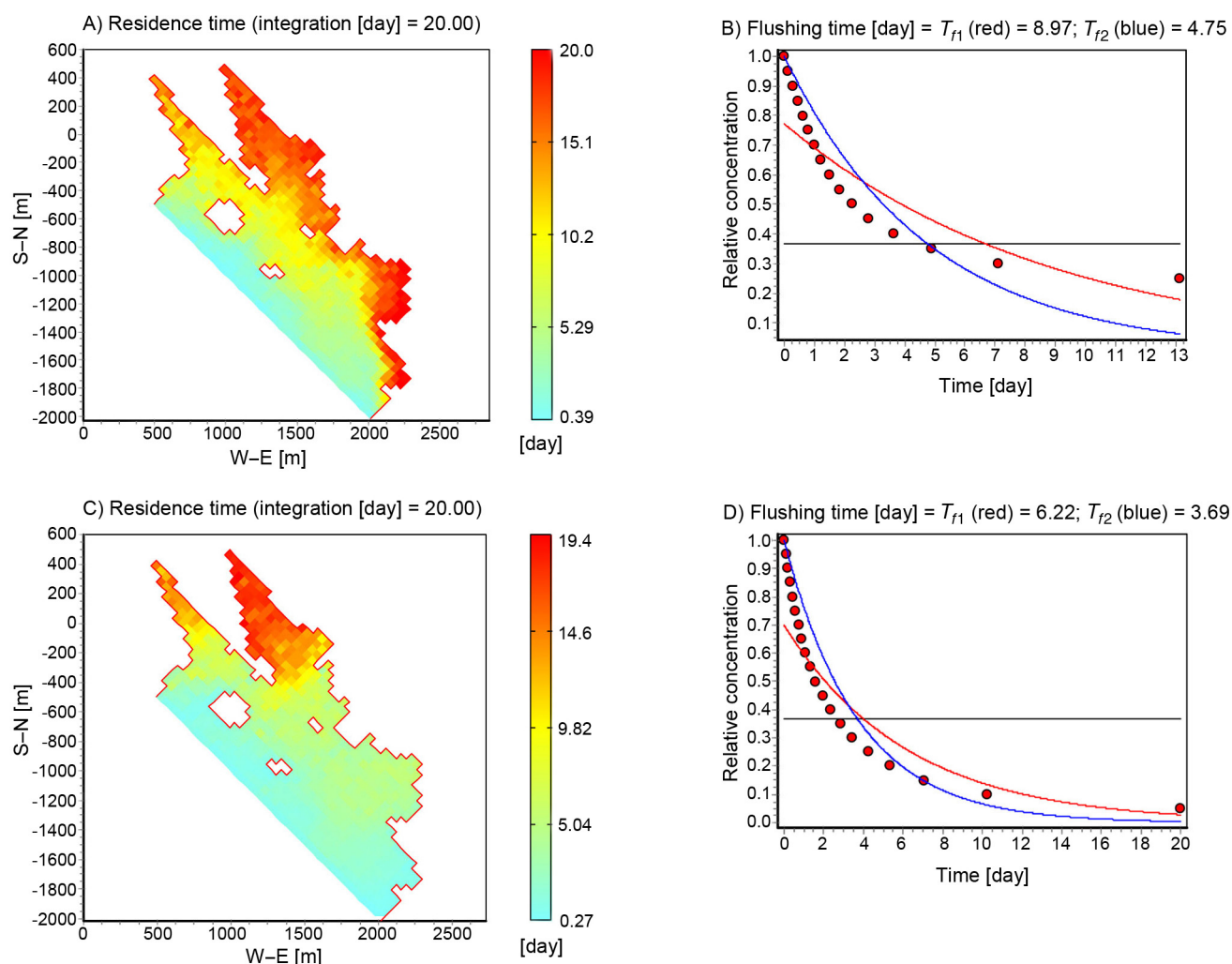
Figure 6   Residence and flushing time estimations for *Maestral* wind (A) and (B), and *Bura* wind (C) and (D).
Redrawn from SUO Lamjana (2011).

removal of scalars from the system. The significance of seabed topography is easily recognizable from hydrodynamic simulation models. The uniform increase in depth and total absence of thresholds or depressions enables unobstructed flow and high flushing efficiency. The simulation model for the predominant *Maestral* wind displays strong current flow starting from the V. Lamjana bay, continuing through the passageway between the islands and cape Zaglavić and exiting the semi-enclosed system SW of the island of Bisage (Fig. 1). This specific hydrodynamic response, verified by the presence of quartz particles in sediments from transects Tr-1 and Tr-2, is of particular interest as the currents create a sort of pathway that starts from the V. Lamjana bay (shipyard) and passes through the areas where FFs A, B and C are located (Fig. 1). The specific topography is also responsible for inducing thermal advection at stations St-1 and St-2, initiating vertical transport from the surface to the bottom by bending the seasonal thermocline in a down-welling motion (Puhr and Pikelj, 2012). The vertical mixing induced by thermal advection reduces OM and TE concentration by transporting the scalars into the bottom waters. The presence of thermal advection was clearly identifiable from sea temperature recorded data measured at St-1 (Fig. 3) and

the elevated concentrations of Zn found in 5 m depth sediment samples from Tr-1 and Tr-2 (Fig. 4). The final EF identified as having a major influence on the OM and TE retention is the sediment mineral composition. The sediment samples mostly contained relatively inert carbonates. Together with quartz and other minerals such as feldspars they form a low adhesive power complex, which in return significantly contributed to the overall low concentrations of OM and TE. The sediment mineral composition significance can be clearly observed in 20 m depth sample from Tr-3 where the highest silt and clay fraction and the lowest sand percentage (Table 1) correlated with the highest recorded OM value (4.1%) and 2 to 6 times higher concentrations of TE than measured in 20 m samples from the other two transects (Table 2).

4.2. Synergic power of the principal EFs

The sum of the individual influence of the principal EFs does not fully explain the uniformity and the surprisingly low values of OM and TE within the sediment samples. This discrepancy could be attributed to the synergic power of the principal EFs that forms due to the semi-enclosed nature

of the research site. Although general attitude toward fish farming would suggest the synergy to amplify (increase) concentrations of OM and TE within the system, the research data indicate a completely inverse effect. The results show that the system is capable of eliminating OM and TE input so effectively that the pressure FFs induce on the ecosystem may be described as minimal. The synergy of the principal EFs can, therefore, be defined as having an attenuating effect which enables the system to tolerate a much higher OM and TE input than expected for semi-enclosed systems. The only factor that can be described as being significantly amplified by the synergy is the spatial footprint. The presence of quartz particles within the sediment samples from transects Tr1 and Tr2 set the shipyard's influence at ≈2000 m distance. This is a highly relevant find as all aquaculture models use much smaller radiuses in assessing the impacted zones. It is clear that the synergic effect is capable of altering the conditions in a way that is favorable for processing aquaculture OM and TE input, but at the same time, it significantly increases their ecological footprint. The fact that shipyard's influence stretched over the FFs at locations A, B and C (Fig. 1) has strongly negative connotations, suggesting that positioning the FF cages "downstream" along the wind induced currents pathway must be avoided regardless of relative distances between installations.

5. Conclusion

The results of the research have provided insight into the problems regarding integration of multiple FFs within semi-enclosed bays. The data indicate that a successful integration of four FFs has taken place within the research domain, and that the key EFs responsible for its success are strong wind induced hydrodynamics, favorable seabed topography and sediment mineral composition. By examining the principal EFs it seems reasonable to assume that the prerequisites for a successful integration could be found in numerous locations across the East Adriatic and the Mediterranean Sea. Although the integration requirements seem straight-forward, it is imperative that the synergic effect is established for each individual case. The fact that so little is known about this phenomenon causes concern since there is no guarantee that the synergy would have the same positive effect at different locations due to its complexity. Therefore, prior to implementation of the presented finds further investigations into the behavior of this factor in correlation to different EFs scales and OM and TE inputs are mandatory.

Acknowledgements

References

Apostolaki, E.T., Núria Marbà, N., Holmer, M., Karakassis, I., 2009. Fish farming impact on decomposition of *Posidonia oceanica* litter. J. Exp. Mar. Biol. Ecol. 369 (1), 58—64, http://dx.doi. org/10.1016/j.jembe.2008.10.022.

Blott, S.J., Pye, K., 2001. GRADISTAT: a grain size distribution and statistics package for the analysis of unconsolidated sediments. Earth Surf. Proc. Land. 26 (11), 1237—1248, http://dx.doi.org/ 10.1002/esp.261.

Blumberg, A.F., Mellor, G.L., 1987. A description of a three-dimensional coastal ocean circulation model. In: Heaps, N.S. (Ed.), Three Dimensional Coastal Ocean Models, Coastal and Estuarine Science 4. Am. Geophys. Union, Washington, DC, 1—16.

Borja, A., German Rodriguez, J., Black, K., Bodoy, A., Emblow, C., Fernandes, T., Forte, J., Karakassis, I., Muxika, I., Nickell, T., Papageorgiou, N., Pranovi, F., Sevastou, K., Tomassetti, P., Angel, D., 2009. Assessing the suitability of a range of benthic indices in the evaluation of environmental impact of fin and shellfish aquaculture located in sites across Europe. Aquaculture 293 (3—4), 231—240, http://dx.doi.org/10.1016/j.aquaculture.2009.04.037.

Cancemi, G., De Falco, G., Pergent, G., 2003. Effects of organic matter input from a fish farming facility on a *Posidonia oceanica* meadow. Estuar. Coast. Shelf Sci. 56 (5—6), 961—968, http://dx. doi.org/10.1016/S0272-7714(02)00295-0.

Clement, D., Keeley, N., Sneddon, R., 2010. Ecological relevance of Copper (Cu) and Zinc (Zn) in sediments beneath fish farms in New Zealand. Report No. 1805, 48 pp.

Cukrov, N., Frančišković-Bilinski, S., Mikac, N., Roje, V., 2008. Natural and anthropogenic influences recorded in sediments from the Krka river estuary (Eastern Adriatic coast), evaluated by statistical methods. Fresenius Environ. Bull. 17, 855—863.

Delgado, O., Grau, A., Pou, S., Riera, F., Massuti, C., Zabala, M., Ballestros, E., 1997. Seagrass regression caused by fish cultures in Fornells Bay, Menorca, western Mediterranean. Oceanol. Acta 20 (3), 557—564, http://archimer.ifremer.fr/doc/00093/20415/.

Dolenec, T., Faganeli, J., Pirc, S., 1998. Major, minor and trace elements in surficial sediments from the open Adriatic Sea: a regional geochemical study. Geol. Croat. 51 (1), 59—73.

Fajković, H., Prohić, E., Abramović, D., 2013. Contamination of seabed sediments around a shipyard in the Adriatic Sea (Ugljan Island). Geol. Croat. 66 (1), 77—82.

FAO FishstatJ, 2012. Aquaculture Production: Quantities 1950—2010, http://www.fao.org/fishery/statistics/software/fishstatj/en.

Fiket, Ž., Mikac, N., Kniewald, G., 2016. Mass fractions of forty-six major and trace elements, including rare earth elements, in sediment and soil reference materials used in environmental studies. Geostand. Geoanal. Res. 41 (1), 123—135, http://dx. doi.org/10.1111/ggr.12129.

Folk, R.L., 1954. The distinction between grain size and mineral composition in sedimentary rock nomenclature. J. Geol. 62 (4), 344—359, http://www.jstor.org/stable/30065016.

Förstner, U., Wittmann, G.T.W., 1983. Metal Pollution in the Aquatic Environment. Springer-Verlag, Berlin/Heidelberg, New York, 481 pp.

Karakassis, I., Tsapakis, M., Hatziyanni, E., Papadopoulou, K.N., Plaiti, W., 2000. Impact of cage farming on fish on the seabed in three Mediterranean coastal areas. ICES J. Mar. Sci. 57 (5), 1462—1471, http://dx.doi.org/10.1006/jmsc.2000.0925.

Karakassis, I., Pitta, P., Krom, M.D., 2005. Contribution of fish farming to the nutrient loading of the Mediterranean. Sci. Mar. 69 (2), 313—321, http://dx.doi.org/10.3989/scimar.2005.69n2313.

Karlsson, J., Ytreberg, E., Eklund, B., 2010. Toxicity of anti-fouling paints for use on ships and leisure boats to non-target organisms representing three trophic levels. Environ. Pollut. 158 (3), 681—687, http://dx.doi.org/10.1016/j.envpol.2009.10.024.

Knauss, J.A., 1978. Introduction to Physical Oceanography. Prentice-Hall, Englewood Cliffs, NJ, 338 pp.

Longstaff, B.J., Dennison, W.C., 1999. Seagrass survival during pulsed turbidity events: the effects of light deprivation on the seagrasses *Halodule pinifolia* and *Halophila ovalis*. Aquat. Bot. 65 (1—4), 105—121, http://dx.doi.org/10.1016/S0304-3770(99)00035-2.

Majcen, Ž., Korolija, B., Sokač, B., Nikler, L., 1970. Basic Geological Map of SFRY 1:100000, Zadar Sheet K 33-139. Geološki zavod, Zagreb, Savezni geološki zavod, Beograd (in Croatian).

Maldonado, M., Carmona, M.C., Echeverria, Y., Riesgo, A., 2005. The environmental impact of Mediterranean cage fish farms at semi-exposed locations: does it need a re-assessment? Helgol. Mar. Res. 59 (2), 121—135, http://dx.doi.org/10.1007/s10152-004-0211-5.

Matijević, S., Bogner, D., Morović, M., Tičina, V., Grbec, B., 2008. Characteristics of the sediment along the eastern Adriatic coast (Croatia). Fresenius Environ. Bull. 17 (10b), 1763—1772.

Miller, R.L., McPherson, B.F., 1995. Modelling photosynthetically active radiation in water of Tampa Bay, Florida, with emphasis on the geometry of incident irradiance. Estuar. Coast. Shelf Sci. 40 (4), 359—377, http://dx.doi.org/10.1006/ecss.1995.0025.

Monsen, N.E., Cloern, J.E., Lucas, L.V., Monismith, S.G., 2002. A comment on the use of Flushing Time, Residence Time and Age as transport time scales. Limnol. Oceanogr. 47 (5), 1545—1553, http://dx.doi.org/10.4319/lo.2002.47.5.1545.

Morse, J.W., Mackenzie, F.T., 1990. Geochemistry of Sedimentary Carbonates. Elsevier, Amsterdam, 185 pp.

Neofitou, N., Klaoudatos, S., 2008. Effects of fish farming on the water column nutrient concentration in a semi-enclosed gulf of the Eastern Mediterranean. Aquacult. Res. 39 (5), 482—490, http://dx.doi.org/10.1111/j.1365-2109.2008.01900.x.

Orlić, M., Pasarić, Z., 2011. A simple analytical model of periodic coastal upwelling. J. Phys. Oceanogr. 41, 1271—1276, http://dx.doi.org/10.1175/JPO-D-10-05000.1.

Papageorgiou, N., Kalantzi, I., Karakassis, I., 2010. Effects of fish farming on the biological and geochemical properties of muddy and sandy sediments in the Mediterranean Sea. Mar. Environ. Res. 69 (5), 326—336, http://dx.doi.org/10.1016/j.marenvres.2009.12.007.

Pergent, G., Mendez, S., Pergent-Martini, C., Pasqualini, V., 1999. Preliminary data on the impact of fish farming facilities on *Posidonia oceanica* meadows in the Mediterranean. Oceanol. Acta 22 (1), 95—107, http://dx.doi.org/10.1016/S0399-1784(99)80036-X.

Pergent-Martini, C., Boudouresque, C.F., Pasqualini, V., Pergent, G., 2006. Impact of fish farming facilities on *Posidonia oceanica* meadows: a review. Mar. Ecol. 27 (4), 310—319, http://dx.doi.org/10.1111/j.1439-0485.2006.00122.x.

Pikelj, K., Jakšić, L., Aščić, Š., Juračić, M., 2016. Characterization of the fine-grained fraction in the surface sediment of the eastern Adriatic channel areas. Acta Adriat. 57 (2), 195—208.

Puhr, K., Pikelj, K., 2012. The effect of *in situ* shading on a *Posidonia oceanica* meadow situated within a fish farm induced moderately nutrient enriched environment. Mar. Pollut. Bull. 64 (8), 1537—1548, http://dx.doi.org/10.1016/j.marpolbul.2012.05.022.

SUO Lamjana, 2011. Zahtjev za ocjenu o potrebi procjene utjecaja na okoliš zahvata dogradnje ribarske luke V. Lamjana, općina Kali, otok Ugljan (in Croatian). Environmental Study. Ekonerg d.o.o. 67.

Takeoka, H., 1984. Fundamental concepts of exchange and transport time scales in a coastal sea. Cont. Shelf Res. 3 (3), 311—326, http://dx.doi.org/10.1016/0278-4343(84)90014-1.

Wu, R.S.S., 1995. The environmental impact of marine fish culture: towards a sustainable future. Mar. Pollut. Bull. 31 (4—12), 159—166, http://dx.doi.org/10.1016/0025-326X(95)00100-2.